Biochimica et Biophysica Acta 1838 (2014) 134–147

Contents lists available at ScienceDirect

Biochimica et Biophysica Acta

journal homepage: www.elsevier.com/locate/bbamem

Improving the stability and function of purified ABCB1 and ABCA4: The influence of membrane lipids

Naomi L. Pollock [a], Christopher A. McDevitt [a], Richard Collins [b], Petronella H.M. Niesten [a], Stephen Prince [b], Ian D. Kerr [c], Robert C. Ford [b], Richard Callaghan [a,d,*]

[a] Nuffield Department of Clinical Laboratory Sciences, John Radcliffe Hospital, University of Oxford, Oxford OX3 9DU, UK
[b] Manchester Interdisciplinary Biocentre, Faculty of Life Sciences, University of Manchester, Manchester M1 7DN, UK
[c] School of Biomedical Sciences, University of Nottingham, Queen's Medical Centre, Nottingham NG7 2UH, UK
[d] Division of Biomedical Science & Biochemistry, Research School of Biology, College of Medicine, Biology & Environment, The Australian National University, Canberra, ACT 0200, Australia

ARTICLE INFO

Article history:
Received 6 May 2013
Received in revised form 27 August 2013
Accepted 3 September 2013
Available online 12 September 2013

Keywords:
ATP Binding Cassette transporter
Membrane transport
Lipid–protein interaction
Membrane protein structure
P-glycoprotein
ABCA4

ABSTRACT

ATP Binding Cassette (ABC) transporters play prominent roles in numerous cellular processes and many have been implicated in human diseases. Unfortunately, detailed mechanistic information on the majority of ABC transporters has not yet been elucidated. The slow rate of progress of molecular and high resolution structural studies may be attributed to the difficulty in the investigation of integral membrane proteins. These difficulties include the expression of functional, non-aggregated protein in heterologous systems. Furthermore, the extraction of membrane proteins from source material remains a major bottle-neck in the process since there are relatively few guidelines for selection of an appropriate detergent to achieve optimal extraction. Whilst affinity tag strategies have simplified the purification of membrane proteins; many challenges remain. For example, the chromatographic process and associated steps can rapidly lead to functional inactivation, random aggregation, or even precipitation of the target protein. Furthermore, optimisation of high yield and purity, does not guarantee successful structure determination. Based on this series of potential issues, any investigation into structure–function of membrane proteins requires a systematic evaluation of preparation quality. In particular, the evaluation should focus on function, homogeneity and mono-dispersity. The present investigation provides a detailed assessment of the quality of purified ATP Binding Cassette (ABC) transporters; namely ABCB1 (P-gp) and ABCA4 (ABCR). A number of suggestions are provided to facilitate the production of functional, homogeneous and mono-disperse preparations using the insect cell expression system. Finally, the ABCA4 samples have been used to provide structural insights into this essential photo-receptor cell protein.

1. Introduction

A recent article has labelled ABC transporters akin to a "*riddle wrapped in a mystery inside an enigma*" due to their wide range of functions and the complexities surrounding their molecular mechanism [1]. However, this label may equally apply to the difficulty in handling ABC transporters and, for that matter, other polytopic membrane proteins. Solving this riddle remains an important research goal, as membrane proteins are the targets for more than 40% of existing pharmacological agents; a testament to their importance in human health.

Molecular mechanisms of proteins involved in transport processes have a number of key steps including (i) substrate binding, (ii) binding site reorientation, (iii) provision of energetics for transport, (iv) coupling substrate binding and energy provision, (v) substrate dissociation, and (vi) re-setting of the transport machinery [2,3]. Elucidation of a mechanism to unite these steps requires a large body of information gleaned from biochemical, pharmacological and structural investigations. No single discipline can generate sufficiently diverse information to provide a unifying mechanism. The process requires a multi-disciplinary approach to the problem. Unfortunately, the pace of different disciplines varies and in the case of ABC transporters, the availability of structural data remains the "slow runner" in generating molecular mechanisms.

The inherent difficulty in attaining high-resolution structural information of membrane proteins can be illustrated by examining the structures deposited in the Protein Data Bank (www.rcsb.org). To date, there are currently 342 high-resolution (i.e. X-ray or NMR based) structures available for membrane proteins and of these less than 200 are polytopic. In contrast, in the first quarter of 2012 alone, over 2000 structures of soluble proteins were deposited into the Protein Data Bank. There are numerous reasons for this lag in membrane protein structural resolution, beginning with difficulties in their over-expression. The plasma (or organelle) membrane has a finite capacity for large polytopic proteins, which limits their heterologous overexpression, compared to that of soluble proteins. Furthermore the cheap, convenient and high-

* Corresponding author at: Building 134, Research School of Biology, The Australian National University, Acton, ACT 0200, Australia. Tel.: +61 2 6125 0824.
E-mail address: richard.callaghan@anu.edu.au (R. Callaghan).

0005-2736/$ – see front matter © 2013 Elsevier B.V. All rights reserved.
http://dx.doi.org/10.1016/j.bbamem.2013.09.001

yield bacterial overexpression systems are significantly less efficient at synthesising proteins with molecular weights greater than approximately 100 kDa. This reduces the choice of expression systems for eukaryotic membrane proteins, and the typical yields for membrane proteins are markedly lower than their soluble peers.

To enable chromatographic purification, membrane proteins must be extracted from their native location. This is commonly achieved using detergents, resulting in the insertion of the protein into a micelle structure [4]. The amphipathic nature of the detergent should enable both the structure and solubility of the protein to be maintained in the solvent environment. Following purification of the protein, crystallisation screening is undertaken, aimed at inducing ordered aggregation of the protein species. However, the physical properties of protein–detergent micelles may hinder the formation of protein–protein contacts that are fundamental to crystal formation. Due to the differing lateral pressure and relatively low structural order, detergent micelles also provide an environment that allows the membrane proteins to adopt multiple conformations. Since these proteins, particularly the transporters, are dynamic structures, the tendency to adopt multiple conformational states may also impair crystal formation.

Retrospective analysis of membrane proteins that have been crystallised provides important guidelines for optimal conditions, or protein quality, required for successful structural determination [5–8]. The yield, concentration and purity of the protein preparations are established requirements for structural studies. However, ascertaining the homogeneity, or monodispersity, should be a primary analytical undertaking for the purified protein. The homogeneity takes into account the aggregation state(s) of a protein, the adoption of multiple conformations, and the variety of protein–detergent micelle structures.

Our investigation has characterised the quality of two purified human ABC transporters, both of which have considerable importance in human health. Currently, there are 9 structures for full-length ABC transporters that have been generated through X-ray crystallography. Of these, only two are mammalian, one of which is ABCB10 [9] and the other a mouse isoform of P-glycoprotein (P-gp or ABCB1) [10]. Recently the structure of a *Caenorhabditis elegans* homologue of ABCB1 has been reported [11]. However, despite attempts from numerous research teams, human ABCB1 has not proven amenable to crystallisation and the reasons underlying this intransigence remain unclear. ABCB1 is the archetypal multidrug efflux pump and is a key determinant of the efficacy of chemotherapy in a number of cancer types [12–14]. In addition, its expression in "normal" (i.e. non-cancer) cells shapes the pharmacokinetic profile for an extraordinary number of pharmaceutical compounds. Our laboratories have generated expression, purification and reconstitution systems for ABCB1 during the last two decades and have invested much effort in optimisation of the protein isolation [15–21]. In addition, our teams have generated the first and most extensive structural data for ABCB1 using electron microscopy and small angle X-ray scattering based approaches [22–24].

In the present article we outline recent attempts to improve the homogeneity and stability of purified human ABCB1 as a firm foundation for future structural studies. In addition, the article presents an equivalent optimisation strategy for the ABC transporter associated with Stargardt disease; namely human ABCA4 protein [25,26]. Considerably larger than ABCB1 (250 vs 140 kDa), ABCA4 is an interesting comparison for the investigations with ABCB1 as it consists of a similar core functional unit of two transmembrane domains (TMDs) and two nucleotide binding domains (NBDs), with the addition of two large soluble domains on the opposite side of the membrane to the NBDs [27]. Moreover, its putative role in retinal-PE flip–flop in the disc membranes of photoreceptor cells would render this protein as the only known human ABC importer.

Our strategy has been to characterise the isolation and stability of ABCA4 and ABCB1 using a mixture of biophysical and functional approaches. In addition, the purified ABCA4 has been used to provide a low-resolution structure using electron microscopy.

2. Materials and methods

2.1. Materials

Trichoplusia ni and *Spodoptera frugiperda* cells, and foetal bovine serum (FBS) were purchased from Invitrogen Ltd (Paisley, UK), ExCell cell culture medium from SAFC (Dorset, UK) and Insect-XPRESS cell culture medium, penicillin–streptomycin (P–S) and SeaPlaque agarose were from Lonza Wokingham Ltd (Berkshire, UK). n-Dodecyl-β-D-maltoside, n-decyl-β-D-maltoside, n-nonyl-β-D-maltoside, Cymal-5, the fos-choline detergents (FC-14 and FC-16) and dodecyldimethylamineoxide (all >99% purity) were from Anatrace (Ohio, US); octyl-β-glucoside and Ni-NTA His-bind Superflow resin were from Merck Biochemicals (Nottinghamshire, UK); complete protease inhibitor tablets were from Roche Diagnostics Ltd (Sussex, UK). Cholesterol (>99% purity), cholesteryl hemisuccinate tris salt, sodium cholate, soy bean asolectin, trypsin and DL-dithiothreitol (DTT) were purchased from Sigma-Aldrich and tris(2-carboxyethyl)phosphine hydrochloride (TCEP) was from Soltec Ventures (Massachusetts, USA). Columns for gel permeation chromatography (Superdex 200 10/300 GL, Superose6 10/300 GL, 5 ml Sephadex-G25 PD10 column) and materials for immobilised metal ion chromatography (5 ml HisTrap columns, Ni-Sepharose Fast Flow resin) were from GE Healthcare Biosciences (Buckinghamshire, UK). Millipore (Hertfordshire, UK) supplied 100 kDa molecular weight cut-off (MWCO) 4 ml and 15 ml centrifugal concentrators, pressure cell concentrators and ultrafiltration membranes. Low volume centrifugal concentrators (Vivaspin 500, 100 kDa MWCO) were from Sartorius Biotechnology Ltd (Surrey, UK). Total *Escherichia coli* lipid extract, total porcine brain lipid extract, and porcine brain phosphatidyl choline (>99% purity) were purchased from Avanti Polar Lipids Inc. (Alabama, US). SM-2 adsorbent polystyrene BioBeads and Econo columns were supplied by Bio-Rad Laboratories (Hertfordshire, UK). Sigma-Aldrich supplied the following nucleotides and nucleotide analogues: adenosine 5′-triphosphate disodium salt hydrate, adenosine 5′-triphosphate magnesium salt (Na_2ATP, MgATP), adenosine 5′-diphosphate disodium salt (ADP), adenosine 5′-(β,γ-imido)triphosphate tetralithium salt hydrate (AMP-PNP), 2′,3′-O-(2,4,6-trinitrophenyl) adenosine 5′-triphosphate monolithium trisodium salt (TNP-ATP). Invitrogen supplied 7-diethylamino-3-(4′-maleimidylphenyl)-4-methylcoumarin (CPM). Acrylamide ProtoGel was obtained from National Diagnostics Ltd (Yorkshire, UK) and PAGE-Blue stain was from Fermentas (Yorkshire, UK). Precision Plus Protein Kaleidoscope Prestained standards and the DC-Bio-Rad protein assay kit were from Bio-Rad Laboratories. Hybond ECL nitrocellulose membrane and the ECL Western Blotting System (chemiluminescent reagents and photographic film) were supplied by GE Healthcare Biosciences. Skimmed milk powder was from Waitrose (Berkshire, UK) and Tween-20 was from Sigma-Aldrich. The monoclonal mouse IgG HRP-conjugated anti-6xHis antibody was from R&D Systems Europe Ltd (Oxfordshire, UK) and the monoclonal mouse IgG C219 antibody was purchased from Merck Biochemicals. [α^{32}P]-8-azido-ATP (575 GBq/mmol) was bought from Affinity Labelling Technologies (Lexington, USA) and [α^{32}P]-ATP (29.6 TBq/mmol) was purchased from PerkinElmer LAS (Beaconsfield, UK). Carbon coated copper EM grids (400 mesh/in.) were from Agar Scientific Ltd (Essex, UK) and uranyl acetate was from Sigma-Aldrich.

2.2. Construction of recombinant baculovirus containing ABCA4 or ABCB1

A C-terminal, dodecahexahistidine (His_{12}) tagged isoform of ABCA4 cDNA was generated from an earlier vector (pFastBac1_ABCA4His_6) when initial studies revealed that this hexahistidine tagged isoform failed to interact strongly with nickel charged affinity resins (data not shown). pFastBac1_ABCA4His_6 contains the cDNA for ABCA4 subcloned in at NcoI and HindIII sites, with an additional, internal NcoI site present 1.1 kilobase pairs (kbp) from the 3′ end of the cDNA. PCR primers 5′-GTGAGGAGCACTCTGCAAATCCGTTCCAC and 5′-GCGGTGT

GAGGTGACCGTCCTGGGCTTGTC were used to amplify the 3′ 1.3 kbp of an untagged ABCA4 cDNA from pRK5_ABCA4 (kindly supplied by Dr. J. Nathans (Johns Hopkins University, Baltimore)). The PCR replaced the stop codon with a BstEII site (underlined), and enabled the sub-cloning of this product into a vector pBlueBac_ABCB1_His_{12} at NcoI/BstEII sites. The latter vector contains the cDNA for human ABCB1 with a BstEII site in frame with a C-terminal His_{12} tag [18]. The 3′ end of ABCA4 containing the His_{12} tag was then sub-cloned back into pFastBac1_ABCA4His_6, generating a plasmid (pFastBac1_ABCA4His_{12}) which was validated by DNA sequencing and shown to encode a C-terminal extension of GHHHHHHTGHHHHHH.

The pFastBac1_ABCA4His_{12} vector was transformed into DH10Bac cells by heat shock transformation and colonies containing recombinant bacmid DNA isolated by blue–white screening. Bacmid DNA was prepared by alkaline lysis and was screened by PCR using bacmid primers (M13F and M13R) in combination with various primers internal to the ABCA4 cDNA. Recombinant bacmid DNA was transfected into Sf9 cell monolayers using Cellfectin (3:1 v/w ratio of Cellfectin to DNA) and initial P1 viruses were harvested 4 days later. The P1 stock was purified to remove any parental baculovirus by a plaque assay and blue–white screen, and the resultant purified recombinant virus was amplified and titred as previously described [28].

A C-terminal, dodeca-histidine tagged ABCB1 isoform was constructed as previously described. The poly-histidine tag was engineered into the cDNA of ABCB1 to contain a human rhinovirus 3C-protease cleavage site.

2.3. Tissue culture and membrane preparation

Sf900 insect cells were routinely grown at 27 °C in Insect-XPRESS medium supplemented with 100 U/ml penicillin and 0.1 mg/ml streptomycin. Cell suspensions (5×10^6 cells/ml) were infected with recombinant baculovirus containing ABCA4 at a multiplicity of infection (MOI) of 5.

ABCB1 was expressed in *T. ni* (Hi5) insect cells as previously described [18]. Briefly, Hi5 cells at a density of 3×10^6 cell/ml were infected with baculovirus containing ABCB1 at a MOI of 5.

Cells (Sf900 or Hi5) were diluted 1:1 and grown for 3–4 days with shaking at 140 rpm at 27 °C. Infected cells were collected by centrifugation and stored as pellets at −80 °C until membrane preparation. Crude membranes were prepared by nitrogen cavitation and ultracentrifugation as previously described [19]. The final membrane preparations were flash frozen in liquid nitrogen and stored at a protein concentration of 20–50 mg/ml at −80 °C for up to 12 months.

2.4. Solubilisation procedures for ABCA4 and ABCB1

All solubilisation screens were carried out in a standard solubilisation buffer of 20 mM MOPS pH 7.4, 200 mM NaCl, 20% (w/v) glycerol, 1.5 mM $MgCl_2$ and 5 mM DTT. This buffer was supplemented with 2% (w/v) detergent and membranes added to a final protein concentration of 5 or 10 mg/ml. This mixture was briefly homogenised and incubated at 4 °C for 60 min with stirring. Following incubation with detergent, insoluble material was removed by ultracentrifugation and the supernatant, containing solubilised proteins, retained for chromatography. The insoluble fraction was re-suspended in 10% (w/v) SDS and diluted to the same volume as the soluble fraction. The efficiency of the solubilisation procedure was monitored by assessing the partitioning of the protein of interest between the soluble and insoluble fractions using a Western blot.

ABCA4 was solubilised for routine chromatography using the standard solubilisation buffer supplemented with 2% (w/v) FC-16. The concentration of total membrane proteins in the solubilisation mixture was 5 mg/ml. In purifications that included lipids the lipid mixtures were dissolved in a solvent of 2:1 chloroform:methanol (v/v). Lipid films were prepared from this solution by evaporating the mixture under vacuum for at least 60 min. The lipid films were re-suspended in solubilisation buffer containing detergent by repeated sonication and vortexing until the lipids were evenly dispersed.

For the routine solubilisation of ABCB1, total *E. coli* lipid extract and cholesterol were mixed in a ratio of 4:1 (w/w) and dissolved in a solvent of 2:1 chloroform:methanol (v/v). Lipid films were prepared from this solution by vacuum evaporation and the films re-suspended in solubilisation buffer containing 2% (w/v) dodecyl-β-maltoside to a final lipid concentration of 0.4% (w/v). Isolated insect cell membranes were added to the detergent–lipid mixture at 5 mg/ml protein. This mixture was stirred at 4 °C for 120 min and solubilised proteins were recovered by ultracentrifugation.

2.5. Purification of ABCA4

ABCA4 membranes containing >500 mg total membrane proteins were purified using a pre-packed 5 ml HisTrap column equilibrated using purification buffer (20 mM MOPS pH 7.4, 200 mM NaCl, 10% (v/v) glycerol) supplemented with 5 mM TCEP, 0.01% FC-16 and lipids were required. Solubilised ABCA4 was loaded onto the column at a flow-rate of 0.5 ml/min. The flow rate was increased to 1.5 ml/min and a step-wise gradient of 40–400 mM imidazole was introduced to wash and elute the protein. At this point, the purification buffer containing FC-16 could be exchanged for a buffer including 0.05% β-dodecylmaltoside (β-DDM). Protein was concentrated by ultrafiltration (100 kDa cut-off, Millipore, UK) to <250 μl. Gel permeation chromatography (GPC) using a Superose 6 10/300 column (Retention volume (Ferritin 440 kDa = 14.8 ml)) was used as the second purification step. Protein was loaded into a 500 μl sample injection loop, injected onto the column and eluted at a flow rate of 0.5 ml/min. Fractions were automatically collected in 0.5 ml aliquots.

2.6. Purification of ABCB1

Supernatants of solubilised ABCB1 were fractionated using a 5 ml HisTrap column with a stepwise gradient from 40 to 800 mM imidazole. Solubilised material was passed through the column at 1 ml/min. The flow-rate was then increased to 3 ml/min for washing and elution phases. Selected fractions were concentrated using centrifugal ultrafiltration concentrators (Millipore, UK, 100 kDa cut-off). GPC was performed in 20 mM MOPS pH 7.4, 200 mM NaCl, 5 mM TCEP, 5% glycerol, 0.02% DDM on a Superdex S200 10/300 column (Void volume = 8.5 ml; Conalbumin (75 kDa) = 15.4 ml) at a flow rate of 0.3 ml/min.

2.7. Buffer exchange

Fractions from metal affinity purifications were eluted in buffer containing 400 mM imidazole. This was removed via buffer exchange into an imidazole-free buffer using a 5 ml Sephadex-G25 PD10 column. The column was equilibrated in standard purification buffer used for ABCA4 or ABCB1 containing the respective detergent but no imidazole. Columns were loaded with protein sample, which typically eluted from the PD10 column between 2 and 4 ml. Fractions containing protein were identified by SDS-PAGE and pooled.

2.8. Thermal stability assay

The thermal stability assay was carried out in a 96-well plate format as previously described [29,30]. Purified protein at 5 mg/ml was diluted into detergent-free purification buffer (20 mM MOPS pH 7.4, 200 mM NaCl, 10% (v/v) glycerol, 5 mM DTT). Additives to this buffer, or alterations from its standard composition, are detailed in the figure legends and text. The fluorescent probe CPM was added to a final concentration of 0.7 μg/ml and the samples incubated at 37 °C in a fluorescent plate reader. Fluorescence was measured every 5 s for 120 min using λ_{ex} = 390 nm and λ_{em} = 450 nm. Fluorescence intensity was plotted directly as a function of time, or converted to stability units using the

following equation: $S \cdot U = [F_{max} - F_{(t)}]/F_{max}$, where $F_{(t)}$ was the fluorescence reading at each time point and F_{max} was the maximum fluorescence for the data set. The rate-constant (k) of the folded protein in each condition was calculated by fitting the data with a single exponential decay curve: $Y = S * e^{-kt} + P$, where Y = stability unit, t = incubation time, S = span of stability units, P = plateau and k = rate constant. The half-life ($t_{1/2}$) was calculated from the rate constant thus: $t_{1/2} = 0.69 / k$.

2.9. ATPase assay — colorimetric method

The ATP hydrolytic activity of ABCB1 was determined by measuring the liberation of inorganic phosphate using a modified [20,28] colorimetric assay [31]. The maximal ATPase activity was measured using 0.5–1 μg purified protein and 2 mM Na_2ATP in ATPase buffer (50 mM Tris·HCl pH 7.4, 150 mM NH_4Cl, 5 mM $MgSO_4$, 0.02% (w/v) NaN_3). Stimulated activity was measured in the presence of 10 μM nicardipine. Samples were incubated in the dark at 37 °C for 20 min and the inorganic phosphate measured as described.

2.10. ATPase assay — radioactive method

ATP hydrolysis was measured for purified ABCA4 by following the formation of [α^{32}P]-ADP from [α^{32}P]-ATP with thin layer chromatography (TLC). Michaelis–Menten parameters of hydrolysis were obtained by incubating ABCA4 (1 μg) with 0–5 mM ATP and a trace amount (74 kBq) of [α^{32}P]-ATP in a 1:1 mixture of purification and ATPase buffers. The total sample volume was 50 μl and samples incubated for 60 min at 37 °C. At 10 min intervals, a 1 μl aliquot was spotted onto a cellulose-PEI TLC plate. TLC was done using 0.5 M LiCl, 1 M formic acid at 20 °C; plates were then dried and exposed to Kodak BioMax MS film. The latter was used to identify bands corresponding to ATP and ADP. The latter were cut out of the plates and radioactivity determined using a scintillation counter. The amount of ADP formed (nmol/mg protein) was plotted as a function of time and the slope of this linear relationship was used to provide the rate of ATP hydrolysis. The rate of hydrolysis was calculated at a number of ATP concentrations and the data used to determine the characteristic parameters of maximal hydrolytic rate (V_{MAX}) and affinity (K_M) for nucleotide.

The effects of retinal derivatives, or nucleotide trapping strategies, on ATP hydrolysis were investigated by incubating protein with a fixed concentration of nucleotide (2 mM ATP and 74 kBq [α^{32}P]-ATP). Additives were dispensed from concentrated stocks to ensure minimal proportion of solvent (<1%). Retinal derivatives were kept as stocks in dimethyl-sulfoxide (DMSO) whilst nucleotides (AMP-PNP) were from 100 mM MOPS pH 7.4 buffer.

2.11. Electron microscopy

Grids were glow-discharged to increase the affinity of the carbon support for the protein sample as previously described [32]. Protein was adsorbed onto the grid and stained with uranyl acetate as previously described [33]. Briefly, grids were placed on a 5 μl drop of protein sample. After removal from the protein droplet, the grid was blotted with Whatman paper to remove excess liquid and washed with H_2O. After blotting to remove excess water, the grid was placed on a 5 μl drop of 4% (w/v) uranyl acetate to overlay the protein layer on the grid with a layer of stain. Excess stain was removed by blotting with Whatman paper. Micrographs were recorded using a JEOL 100 kV transmission electron microscope connected to a 3 k × 2 k Gatan CCD camera (University of Manchester) at a magnification of 150,000. Particles were automatically boxed and classified using the EMAN processing suite as previously described [33,34].

Twenty-five well defined and different projection averages from these classes were used to generate an unsymmetrised 3-D volume which was refined and produced a 3-D structure with a clear C2 dimeric appearance (data not shown). This structure was re-refined with C2 symmetry, to reconstruct a 3D volume of the complex at a final resolution of 26 Å. Back projections from this 3D model had a clear correspondence with the class averages and raw particle images, and did not exhibit any initial model dependence.

2.12. Data analysis

All investigations were undertaken with a minimum of three independent protein purifications and date represent mean ± SEM. Statistical analyses were done using GraphPad Prism 4.0 and a P-value < 0.05 was considered significant. Linear and non-linear regression analyses were also performed using this program.

3. Results

3.1. Expression and solubilisation of ABCA4

In contrast to ABCG2 and ABCB1, which demonstrate high level expression of full-length protein in High 5 insect cells [19,35], ABCA4 was reproducibly truncated to 160 kDa in this cell line. There was no such problem in Sf900 cells (Sf9 cells grown in the absence of serum) with high expression in crude membranes at the expected molecular weight of 250 kDa. The membrane yield from a 1 litre culture of Sf900 cells was 156 ± 16 mg protein.

A range of conventional detergents, that have demonstrated wide applicability to membrane proteins, were chosen to extract ABCA4 from crude Sf900 membranes (Fig. 1a). This strategy involved collection of detergent soluble protein in supernatants following 60 min extraction in surfactant concentrations in excess of their CMC. As shown in Fig. 1a, none of the detergents tested were able to effect extraction of ABCA4. The data in Fig. 1a was achieved using a total protein concentration of 10 mg/ml but similar observations were made at 1 mg/ml, which would be expected to facilitate extraction due to the higher detergent:membrane ratio. Similarly, using elevated temperatures (37 °C) or longer incubation periods (up to 24 h) also failed to facilitate the extraction of ABCA4 (data not shown). SDS was utilised in the screens and this strong ionic detergent readily extracted ABCA4 from the Sf900 membranes. A large range of stronger non-ionic and zwitterionic detergent species were subsequently examined (Fig. 1b). The phosphocholine (FC) detergents proved considerably more adept at extracting ABCA4 from Sf900 membranes. The short chain FC-8 species extracted approximately 20% of ABCA4 (data not shown) and the solubilised fraction of the protein was increased to greater than 60–70% with the longer chain length of FC-14 and FC-16. Similar results were obtained using a low initial membrane concentration although a small proportion of the ABCA4 always remained in the detergent insoluble pellet.

Fig. 1c shows that the presence of the reducing agent DTT played a major role in the determining the efficiency of ABCA4 extraction. Even at a FC-14 concentration of 2% (w/v) there was no extraction of ABCA4 in the absence of 2.5 mM DTT (Fig. 1c). In contrast, the presence of reducing agent supported efficient extraction of ABCA4. The data obtained in Fig. 1a–b was obtained in the presence of DTT and all subsequent investigations were under reducing conditions. The biophysical properties of FC detergents are not well described and the use of mixed micelles in the presence of the more conventional (e.g. DDM) detergent was explored. As expected, ABCA4 was extracted in the presence of 2% (w/v) FC-14 (Fig. 1d). Rather surprisingly, the inclusion of 1% (w/v) DDM abrogated the extraction of ABCA4 and even increasing the surfactant concentration to 2% (w/v) failed to improve solubilisation. The underlying reason for this unwanted interaction between the detergents was unexplained and similar results were obtained with the substitution of OG for DDM, or the substitution of FC-16 for FC-14 (data not shown).

Thus, ABCA4, like several ABC transporters, is difficult to extract from insect cell membranes and the optimal conditions to effect solubilisation

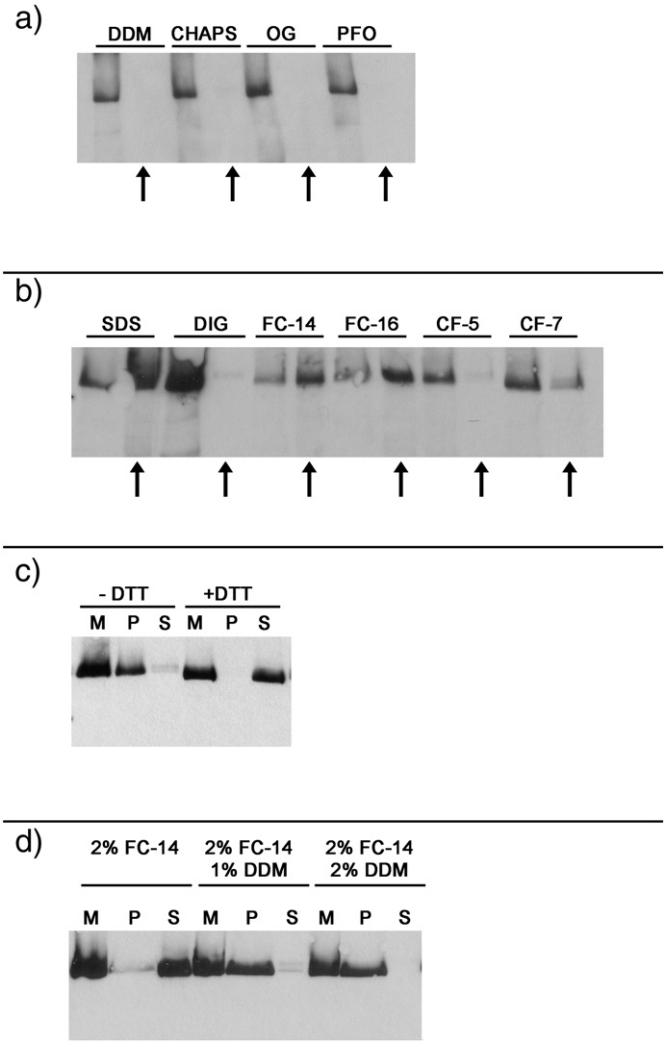

Fig. 1. Solubilisation of ABCA4 from Sf9 insect cell membranes. Insect cell membranes (10 mg/ml) were incubated in the presence of 2% (w/v) of a range of detergent species for 60 min. Solubilised proteins were harvested by ultra-centrifugation at 100,000 ×g for 30 min. Pellets were solubilised in the presence of 2% (w/v) SDS and fractions of both were examined by SDS-PAGE and immuno-blotting. a) Detergent species used were dodecyl-β-maltoside (DDM), CHAPS, octyl-glucoside (OG) and perfluoro-octanoic acid (PFO). Arrows refer to supernatant fractions following ultra-centrifugation, whereas unmarked lanes contain proteins in the pellet. b) Detergent species used were digoxin (DIG), fos-choline 14 (FC-14), fos-choline 16 (FC-16), cyclofos 5 (CF-5), cyclofos 7 (CF-7) and sodium dodecyl-sulphate (SDS) as a positive control. Arrows refer to supernatant fractions following ultra-centrifugation, whereas unmarked lanes contain proteins in the pellet. c) Membranes were treated with FC-14 in the presence or absence of 2.5 mM DTT. Lane assignments are: M — membranes, P — pellet following ultra-centrifugation and S — supernatant following ultra-centrifugation. d) Membranes were treated with FC-14 in the absence or presence of DDM (1–2% w/v). Lane assignments are: M — membranes, P — pellet following ultra-centrifugation and S — supernatant following ultra-centrifugation.

of ABCA4 were: 1.5% (w/v) FC-16 at a membrane protein concentration of 10 mg/ml for 60 min at 4 °C, under reducing conditions. These initial solubilisation conditions were utilised in all subsequent purification procedures with ABCA4.

3.2. Purification of ABCA4 using metal affinity chromatography

ABCA4 had been engineered with a dodeca-histidine tag to enable chromatographic separation using metal affinity chromatography with Ni-NTA resin. Initial studies with a hexa-histidine tag failed to generate protein of sufficient purity (<60%) and were discontinued in favour of the dodeca-histidine isoform. The FC-16 solubilised Sf900 membranes were applied to the Ni-NTA resin at a reduced flow rate to maximise binding of poly-histidine containing proteins. As shown in Fig. 2a there was no ABCA4 in the initial flow through fractions, as detected by PageBlue staining. The initial washing stages of chromatography progressed from 0 to 80 mM imidazole and in order to elute the high affinity binding of ABCA4, the imidazole concentration was raised to 250 mM. ABCA4 eluted at 250 mM imidazole with a purity of approximately 80–85%.

3.3. Purification of ABCB1 using metal affinity chromatography

Since many isoforms of ABCB1 expressed in insect cells were known to solubilise well in DDM, extensive screening of detergents was not carried out for ABCB1. However, we did observe an apparent inverse relationship between the duration of the expression and the detergent "extractability" of ABCB1, with 48–60 hour incubation post-infection being a suitable compromise. Fig. 2b demonstrates the progression of ABCB1 (containing a protease cleavage site for the C-terminal dodeca-histidine tag) purification using an automated chromatography system, which has not previously been shown from our laboratory. The ABCB1 was eluted by an imidazole concentration of 400 mM and the purity following chromatography with the HisTrap resin was approximately 70–75% (estimated by densitometric analysis). The gel in panel b was over-exposed to reveal minor contaminants; with the most common bands at approximately 50 kDa and 80 kDa detected by C219, the monoclonal antibody to ABCB1 (data not shown). These minor contaminating bands were not observed following gel permeation chromatography.

3.4. Analysis of ABCB1 and ABCA4 homogeneity by gel permeation chromatography

The metal affinity chromatography steps described above generated ABCB1/ABCA4 preparations that had purity of approximately 80%. Modifying the metal affinity chromatography conditions did not achieve sufficient improvement in purity. Consequently, an additional purification

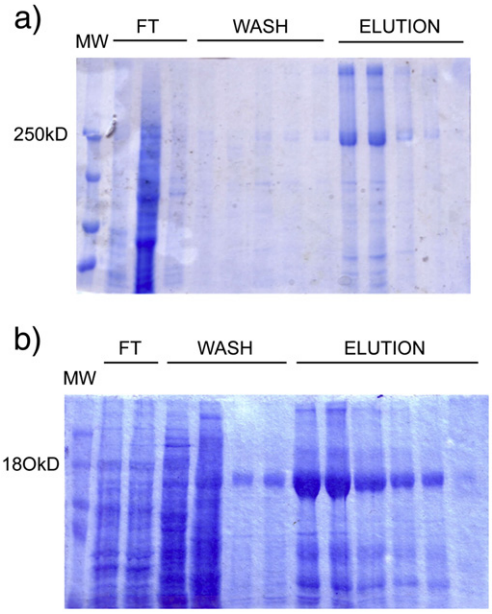

Fig. 2. Chromatographic purification of ABCA4 and ABCB1. Solubilised proteins were separated using IMAC and GPC. Columns were washed in increasing concentrations of imidazole and fractions collected at each stage. a) Metal affinity purification of ABCA4. The Ni-NTA resin was washed in 0–100 mM imidazole and ABCA4 was eluted in the presence of 250 mM imidazole. b) Metal affinity purification of ABCB1. The Ni-NTA resin was washed in 10–100 mM imidazole and ABCB1 was eluted in the presence of 400 mM imidazole. Representative fractions from the flow-through (FT), wash and elution stages of Ni-NTA chromatography were analysed by SDS-PAGE with protein detection using PageBlue reagent. Fractions containing ABCA4 or ABCB1 were pooled and concentrated.

step, gel permeation chromatography (GPC), was incorporated. Another advantage of GPC is the ability to exchange buffer composition to one more compatible with structural or functional investigation; in particular, the removal of the high concentration of imidazole (400 mM). GPC also provides a convenient measure of the homogeneity or mono-dispersity of the purified protein preparations and enables the removal of aggregated species. Prior to GPC, the transporters were concentrated using centrifugal concentrators as described in the Materials and methods section.

ABCA4 (M_W ~ 250 kDa) was subjected to GPC using a Superose 6 column, which has an optimal separation range for soluble globular proteins of 5–5000 kDa. A typical GPC profile (i.e. UV absorbance at 280 nm) for ABCA4 is shown in Fig. 3a (solid line) and samples corresponding to elution volumes of 6–12 ml were analysed by SDS-PAGE (Fig. 3c). The GPC profile revealed two major peaks; one at R_V = 8 ml and another broader peak between R_V = 9–12 ml. The SDS-PAGE analysis indicated that ABCA4 was observed in every fraction from 7 ml to 12 ml and ran at its predicted monomeric molecular weight of ~250 kDa. However, fractions at R_V = 7–9 ml also contained protein at higher molecular weight that barely penetrated the 6% acrylamide gel. Immuno-blotting of the gels indicated that these higher molecular weight bands also contained ABCA4. Any ABCA4 eluting at R_V = 7–9 ml, which corresponds to the column void volume, is likely to be irreversibly aggregated protein. The strength of the aggregation was confirmed by the lack of disruption by SDS and reducing agents in the electrophoresis step. In summary, the combination of GPC and electrophoresis revealed that the ABCA4 preparations contained significant heterogeneity.

GPC of IMAC-purified ABCB1 (M_W ~ 140 kDa) was performed with a Superdex 200 column, which has a resolving range of 3–600 kDa. Fig. 3b (solid line) shows the GPC profile for ABCB1 with the SDS-PAGE analysis of fractions corresponding to R_V = 6–12 ml (Fig. 3d). The GPC profile for ABCB1 also contained two poorly resolved peaks (R_V 8 ml and 11.5 ml respectively), and the protein was observed in all fractions. The earlier peak at R_V = 8 ml contains higher molecular weight forms of ABCB1, which are most likely aggregated protein. The lack of complete resolution between the two ABCB1 containing peaks meant that the final samples were not mono-disperse and contained significant heterogeneity.

3.5. Do buffer components affect the homogeneity of ABCA4 and ABCB1?

The involvement of buffer components in maintaining homogeneity and mono-dispersity of purified proteins is widely recognised. Consequently, preparation of purified proteins and their subsequent crystallisation requires considerable screening of buffer components for their effects on protein state. Of the components used in our buffers for membrane protein purification the imidazole present in the elution fractions was not a requirement thereafter. Consequently we sought to ascertain the effect of the high imidazole concentration on protein state by using buffer exchange (PD-10 column) immediately following metal affinity chromatography prior to concentrating the protein sample for GPC. The resultant GPC profiles for ABCA4 concentrated with and without imidazole are shown in Fig. 3a. The removal of imidazole (dotted line) considerably improved the GPC profile characterised by a major peak at R_V =10.7 ml. This fraction of ABCA4 overlaps directly with the peak obtained in the presence of imidazole. A small "shoulder" peak remained in the region of the void volume and although this peak contained aggregated ABCA4, it accounted for only a minor fraction of the sample.

The comparative GPC profiles for ABCB1 obtained in the presence or absence of imidazole at the concentration step are shown in Fig. 3b. Both spectra contained a major peak eluting at R_V = 11.5 ml, which is believed to correspond to mono-disperse ABCB1. The proportion of ABCB1 found in the peak fraction of the void volume (i.e. R_V = 8 ml) was considerably reduced by removal of imidazole in the buffer.

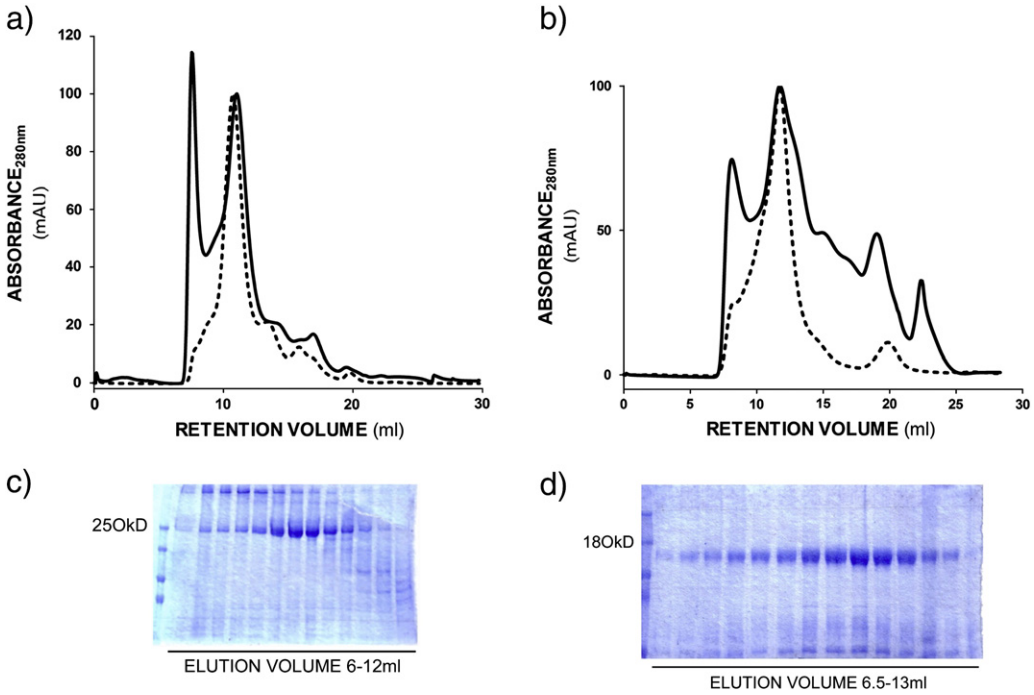

Fig. 3. Effects of imidazole on the homogeneity of ABCB1 and ABCA4. Typical GPC traces are shown for (a) ABCA4 and (b) ABCB1 obtained in the absence (dashed lines) and presence (solid lines) of imidazole. The imidazole was used in eluting protein from Ni-NTA resin and removed, where necessary, using PD-10 columns. Proteins were identified by absorbance at 280 nm using the chromatography system flow cell. Spectral intensities for each trace were normalised with the assignment of the main peak intensity for ABCA4/ABCB1 to 100. ABCA4 and ABCB1 were resolved on Superose 6 and Superdex 200 columns respectively. (c) Concentrated, purified ABCA4 was subjected to gel permeation chromatography on a Superose 6 column. Representative fractions are shown for the void and included fractions. (d) Concentrated, purified ABCB1 was subjected to gel permeation chromatography on a Superdex 200 column. Representative fractions are shown for the void and included fractions.

The data demonstrates the importance of buffer components in dictating the state of purified proteins and supports screening to ensure quality of preparations. In the case of ABCA4 and ABCB1, high concentrations of imidazole should be removed immediately following metal affinity chromatography to prevent aggregation of purified protein. Finally, the use of GPC also improved the purity of the final preparations for both proteins and the combined strategy is a powerful mechanism to achieve mono-dispersity.

3.6. Does storage of ABCB1 and ABCA4 adversely affect the sample homogeneity?

Purification of membrane proteins for long-term structural projects inevitably requires storage of purified protein. Indeed, structural studies involve extended incubation to promote crystal growth. Consequently, the effects of prolonged storage of ABCA4 and ABCB1 were investigated using GPC as a measure of the sample homogeneity. Both proteins were purified using the combination of metal affinity chromatography and GPC as described in the previous sections, with imidazole removed following metal affinity chromatography.

Purified ABCA4 was stored at 4 °C in the dark for a period of 7 days and a sample analysed by GPC. The chromatographic profile for protein prior to, and following, storage at 4 °C is shown in Fig. 4a. The ABCA4 peak was near symmetrical with a $R_V = 11$ ml and there was no alteration in peak symmetry or retention volume following prolonged storage at 4 °C. In addition, there was no alteration in the amount of protein found within the void volume, which indicates minimal aggregation in the buffer system employed for the storage. There was an increase in the peak at $R_V = 20$ ml, however this did not correspond to any protein-based material.

Purified ABCB1 was also subjected to the same storage conditions and the effects on the GPC profile are shown in Fig. 4b. The GPC profile for protein stored for 7 days at 4 °C was similar to that of protein immediately after metal affinity chromatography. The GPC profile offered little evidence of aggregation in the sample; the size, shape and retention volume of the principal peak were largely unchanged between the two conditions. There was a small increase in the amount of material eluting at higher retention volumes (~17.5 ml). These peaks correspond to lower molecular weight species and are thus likely to be proteolytic fragments of ABCB1 that were liberated following storage for 7 days at 4 °C. ABCB1 was also flash frozen in liquid nitrogen and stored at −80 °C for 7 days. The GPC profile revealed that the sample had less evidence of low molecular weight species at $R_V = 17.5$ ml. However, there was a noticeable increase in the amount of protein eluting in the void volume (Fig. 4b), which is indicative of aggregation propensity. These data indicated that protein storage is an important consideration as a freeze–thaw cycle for ABCB1 appeared to induce aggregation, whereas storage at 4 °C resulted in minor degradation.

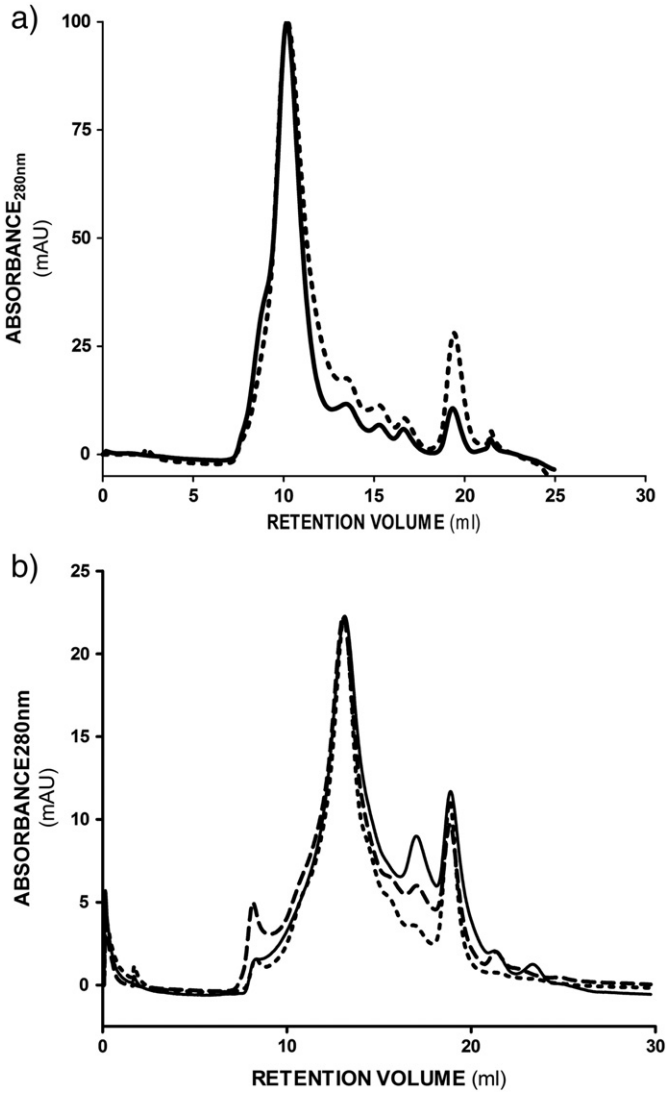

Fig. 4. Effects of storage conditions on protein homogeneity. a) Purified ABCA4 samples were passed through PD-10 columns to remove imidazole. A fraction of the sample was subjected to GPC chromatography (Superose 6) immediately and the resultant profile shown in solid line. Another aliquot of the protein was stored at 4 °C for 7 days, subjected to GPC and the profile shown with a dotted line. b) Purified ABCB1 samples were passed through PD-10 columns to remove imidazole. A fraction of the sample was subjected to GPC chromatography (Superdex 200) immediately and the resultant profile shown in solid line. Another aliquot of the protein was stored at 4 °C for 7 days, subjected to GPC and the profile shown with a dotted line. A further aliquot was flash frozen and stored at −80 °C for 7 days, subjected to GPC and the profile shown with a dashed line.

3.7. The use of an isothermal stability assay to assess protein stability

Detergent extraction of membrane proteins may have severe consequences for protein activity and overall stability, particularly if the process removes annular lipids. The inclusion of "stabilising agents" such as lipids and osmo-protectants may afford increased stability to the isolated proteins. Based on this information, screening additives to improve protein integrity is a hallmark feature of most structural initiatives.

The thermal stability assay provides a rapid and high capacity system to screen stabilising additives. In the present investigation an isothermal version of the assay was adopted. Purified ABCB1 and ABCA4 were incubated in the presence or absence of stabilising compounds at an elevated temperature. The latter induces gradual protein unfolding (i.e. denaturation) and increases access to amino-acid residues previously buried or shielded from the solvent. Addition of the thiol-reactive coumarin, CPM, will provide rapid covalent labelling of exposed cysteine residues. Upon covalent attachment, CPM displays increased fluorescence and the rate of incorporation into the proteins was used to reflect structural destabilisation.

A typical CPM labelling profile for ABCA4 is shown in Fig. 5a over a 2 hour incubation period at 40 °C. The fluorescence increased in a hyperbolic manner and was transformed into a stability curve as seen in Fig. 5b. The stability at the start of the incubation period was assigned a value of 1.0 and a half-life for the decay associated with denaturation was generated from this plot. ABCA4, purified in FC-16 containing buffer was characterised by a denaturation half-life of 15.4 ± 5.7 min and several additives and buffer conditions were examined for their ability to alter this value. A selection of the additives investigated is shown in Fig. 5c. The crude lipid mixture asolectin significantly increased the half-life to 44.8 ± 2.0 min ($P < 0.05$), indicating an improved stability of the protein. Similarly, a mixture of *E. coli* crude lipid extract and cholesterol (4:1 w/w) also increased the stability of ABCA4 with a 2.9-

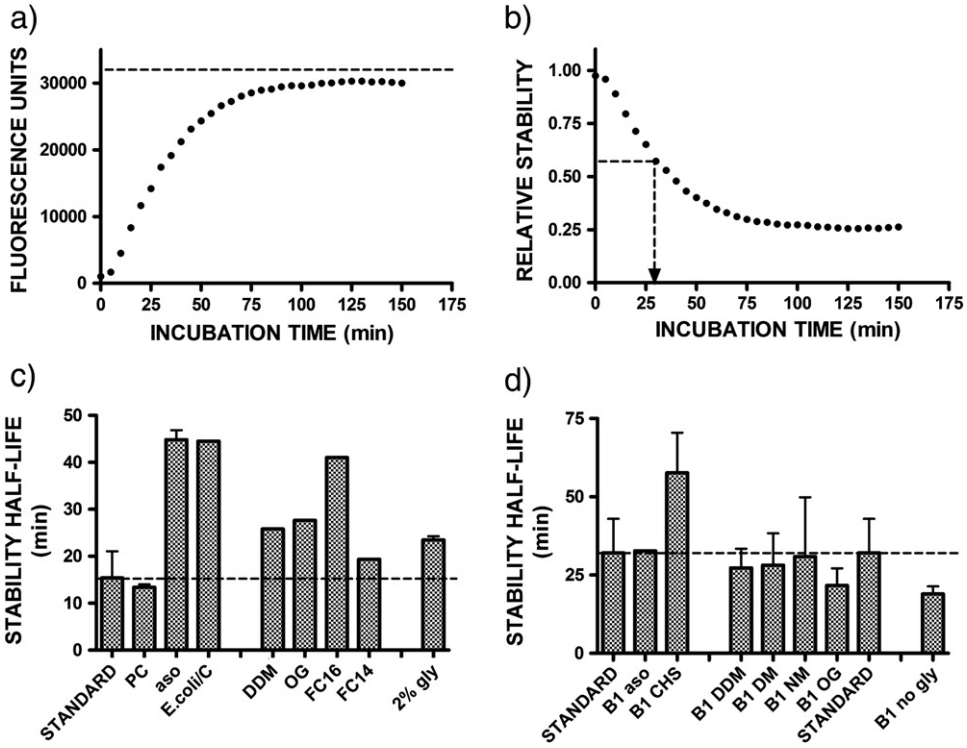

Fig. 5. Using the thermal stability assay to assess the effects of additives on protein stability. Concentrated, purified protein was diluted into a range of purification buffers and its thermal stability at 40 °C was measured using a coumarin–maleimide (CPM) binding assay. Each purification buffer was based on a composition of 20 mM MOPS pH 7.4, 200 mM NaCl and 10% (v/v) glycerol. For ABCA4 the buffer included 0.01% (w/v) FC-16 and for ABCB1 the detergent was 0.05% (w/v) DDM. a) The panel shows the increase in fluorescence during a typical incubation of ABCA4 with CPM under standard conditions over a 150 minute period. The dashed line represents the maximal fluorescence intensity. b) The fluorescence data of panel a) was normalised by expressing as a fraction of the maximal fluorescence intensity. The dashed line demonstrates the interpolation to generate a half-life for the covalent attachment of CPM to ABCA4. c) The half-life for labelling of ABCA4 in the presence of a series of additives. The additives include: PC (addition of 0.1% phosphatidyl choline); aso (addition of 0.1% soy bean asolectin); *E. coli*/cholesterol (addition of 0.16% (w/v) *E. coli* lipids and 0.04% (w/v) cholesterol); DDM, OG, FC16, FC14 (omission of 0.01% (w/v) FC-16, inclusion of dodecylmaltoside, octylglucoside, fos-choline 16 or fos-choline 14 at 3-times their critical micelle concentration); and 2% gly (substitution of 10% (v/v) glycerol for 2% (v/v) glycerol). The protein in its standard buffer is shown and the horizontal dashed line provides another representation of this value for comparison with the other buffer conditions. d) The half-life for labelling of ABCB1 in the presence of a series of additives. The additives include: aso (addition of 0.1% (w/v) soy bean asolectin); CHS (addition of 0.01% (w/v) cholesterol hemi-succinate); DDM, DM, NM, OG (omission of 0.05% (w/v) dodecyl-β-D-maltoside, and inclusion of dodecyl-β-D-maltoside, decyl-β-D-maltoside, nonyl-β-D-maltoside or octylglucoside, at 3-times their critical micelle concentration); and no gly (omission of 10% (v/v) glycerol). The protein in its standard buffer is shown and the horizontal dashed line provides another representation of this value for comparison with the other buffer conditions.

fold increase in the half-life to 44.5 ± 1.0 min. In contrast, the addition of pure phosphatidyl-choline did not alter the stability of ABCA4.

ABCA4 was purified in FC-16 and increasing the detergent concentration from 0.01 to 0.03% (w/v) produced a 2.6-fold increase in the half-life; whereas the inclusion of the shorter alkyl-chain (and higher CMC) FC-14 did not alter the stability. The alkyl-maltoside (DDM) and alkyl-glucoside (OG) detergents also conferred increased stability to the purified protein with elevations in the half-life to 25.8 and 27.6 min respectively. These results indicated that despite the difficulty in solubilising the protein from insect cell membranes, purified ABCA4 was thermally stable in a range of detergents.

Finally, reduction of the concentration of osmo-protectant glycerol in the buffer from 10% (v/v) to 2% (v/v) did not significantly alter the stability of ABCA4. This suggested that ABCA4 could tolerate a reduced glycerol concentration, which is of considerable benefit in crystallisation procedures.

The denaturation of ABCB1 at 40 °C in the DDM containing purification buffer was characterised by a half-life of 32 ± 11 min. The addition of related detergent species, with variable alkyl chain lengths, did not significantly alter the denaturation half-life of ABCB1 (Fig. 5d). The purified protein also had acceptable thermal stability in buffer with glycerol at <10% (v/v) and even in the absence of osmo-protectant the half-life was only reduced to 19 ± 2 min. This condition is essential for analytical methods which require low viscosity such as SAXS, SANS, and static light scattering.

The only additive to significantly increase the mean thermal stability of ABCB1 was 0.01% (w/v) cholesteryl hemisuccinate (CHS). The addition of CHS increased the denaturation half-life from 32 ± 11 min to 58 ± 13 min and indicates stabilisation of the protein in the presence of exogenous cholesterol derivative.

3.8. Does increased stability afforded by lipid derivatives equate to improved homogeneity?

The inclusion of crude lipid mixtures or CHS was shown to improve the structural stability of ABCA4 and ABCB1 respectively. GPC was used to ascertain whether the lipid based additives produced further improvement in the homogeneity of the purified proteins. Both proteins were purified as described previously with the lipid additives included from the solubilisation step and retained throughout the procedure.

Fig. 6a demonstrates the GPC profile obtained for ABCA4 purified in 0.01% FC-16 in the presence or absence of 0.1% (w/v) asolectin. In the absence of added lipid, the ABCA4 protein profile was characterised by a large and nearly symmetrical peak at a $R_V = 11$ ml. However, the inclusion of asolectin during purification produced a rather complex GPC profile. A significant amount of the protein was located within the void volume with a $R_V = 8$ ml, which is suggestive of increased aggregation. In addition, there was no major peak at $R_V = 11$ ml although a large peak was found at $R_V = 9.2$ ml. Finally, a peak corresponding to lower molecular weight at a $R_V = 15$ ml was also observed. Although the structural stability of ABCA4 was improved by the inclusion of crude lipids, the GPC analysis suggested that the protein was found in multiple configurations. The states presumably reflect aggregation of the protein and/or a significantly modified detergent–lipid micelle

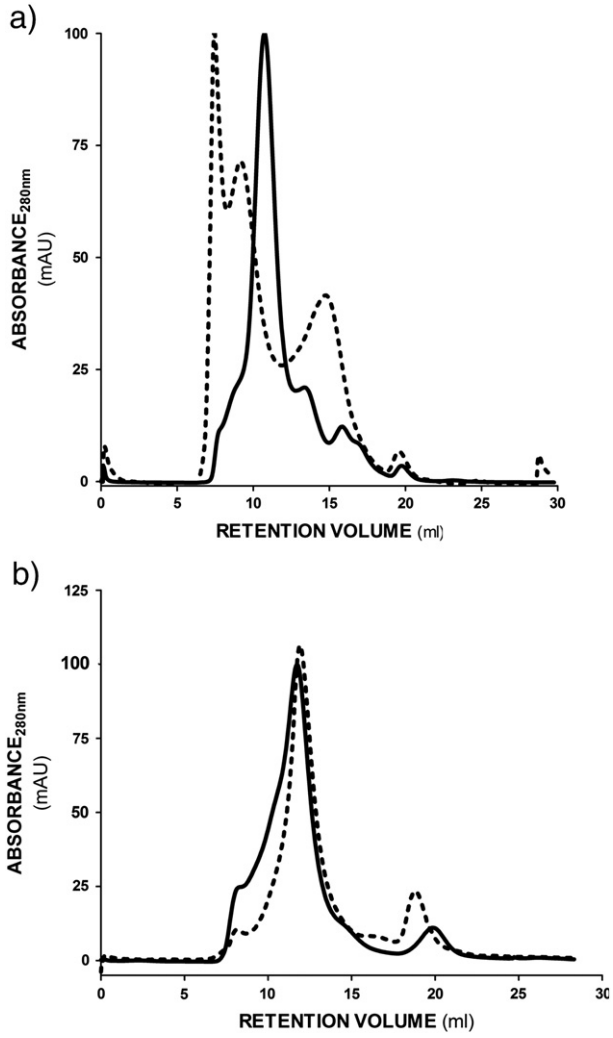

Fig. 6. Effects of exogenous lipids on the homogeneity of ABCB1 and ABCA4. Typical GPC traces are shown for (a) ABCA4 and (b) ABCB1 obtained in the absence (solid lines) and presence (dashed lines) of exogenous lipids. Imidazole used in eluting protein from Ni-NTA resin and was removed using PD-10 columns. The exogenous lipid used in ABCA4 purification was 0.1% (w/v) asolectin. The exogenous lipid used in the purification of ABCB1 was 0.01% (w/v) CHS. Proteins were identified by absorbance at 280 nm using the chromatography system flow cell. Spectral intensities for each trace were normalised with the assignment of the main peak intensity for ABCA4/ABCB1 to 100. ABCA4 and ABCB1 were resolved on Superose 6 and Superdex 200 columns respectively.

containing the ABCA4. Attempts to switch the detergent species from the zwitterionic FC-16 to the non-ionic DDM also produced a complex GPC profile with multiple peaks at a range of retention volumes (data not shown). One interpretation is that ABCA4 adopts a number of configurations when isolated from biological membranes and the simple single detergent system without lipids is more likely to promote mono-dispersity.

Fig. 6b provides the GPC profile for ABCB1 purified in the presence or absence of 0.01% (w/v) CHS using the detergent DDM (0.05% w/v). As described in a previous section, the main peak for ABCB1 (R_V = 11.5 ml) contained a small shoulder peak from the void volume that caused an asymmetric appearance. Inclusion of CHS greatly improved the GPC profile by reducing the proportion of protein contained within the void volume and thereby rendering the peak more symmetric. Thus, the combination of removing imidazole and the inclusion of CHS produced significant improvements in the homogeneity of purified ABCB1; in particular, this strategy reduced the amount of protein appearing in a high molecular weight aggregated state.

3.9. Does increased structural stability afforded by lipid derivatives equate to improved activity of ABCB1?

The inclusion of CHS resulted in increased structural stability and greater homogeneity for ABCB1 following purification. The procedure involved four discrete stages: (a) metal affinity chromatography, (b) removal of imidazole using PD-10 columns, (c) centrifugal concentration, and (d) GPC. The ATPase activity of ABCB1 was measured following each of these treatments to assess their effects on activity and the ability of CHS to prevent any perturbation.

The activity of ABCB1 following metal affinity chromatography in the absence of CHS was characterised with a basal V_{MAX} = 3.3 ± 1.6 nmol/min/mg and this was stimulated 3-fold by nicardipine (10 μM) to V_{MAX} = 9.9 ± 2.9 nmol/min/mg. Progression of the sample through subsequent stages of purification did not see any alteration in this low level of basal or stimulated activity (Fig. 7).

In the presence of CHS, the basal ATPase activity was raised to V_{MAX} = 14 ± 5 nmol/min/mg and the stimulated activity was increased 11-fold to V_{MAX} = 110 ± 46 nmol/min/mg (Fig. 7). Removal of imidazole did not have a significant impact on the basal (V_{MAX} = 21 ± 5 nmol/min/mg) or nicardipine stimulated (V_{MAX} = 97 ± 32 nmol/min/mg) ATPase activity. However, the centrifugal concentration step was associated with a drop in the drug stimulated activity to V_{MAX} = 43 ± 18 nmol/min/mg indicating some inactivation of the protein. Notwithstanding this, the data in this investigation reveals a key role for a cholesterol derivative in maintaining stability and homogeneity of the protein following extraction from the lipid bilayer.

The ATPase activities were determined using ABCB1 in detergent micelle suspensions since this is the form used in structural and many biophysical applications. We have previously demonstrated that human [19,36] and hamster [37] isoforms of ABCB1 display considerable increase in ATPase activity following reconstitution into specific bilayer environments.

3.10. Does increased structural stability afforded by lipid derivatives equate to improved activity of ABCA4?

Crude lipid mixtures were also shown (Fig. 5c) to increase the structural stability, though not the mono-dispersity, of ABCA4. Consequently, the ability of a variety of lipid species to support the ATPase activity of

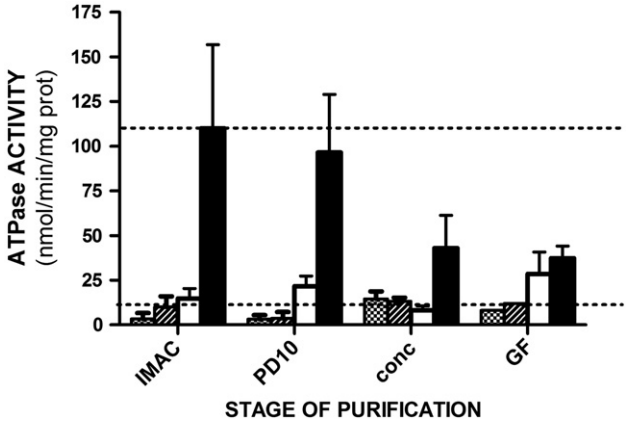

Fig. 7. Effects of CHS on ATP hydrolysis by ABCB1. The ATPase activity of ABCB1 was measured at the following stages of purification: (i) post-metal affinity chromatography, (ii) after removal of imidazole using a PD-10 column, (iii) after centrifugal concentration and (iv) following gel permeation chromatography. The ATPase activity was measured from 200 ng purified ABCB1 incubated at 37 °C for 20 min. The hydrolysis of ATP was detected by the liberation of free phosphate using a colorimetric assay as described in the Materials and methods section. Stimulated activity was measured in the presence of 10 μM nicardipine. Activities were measured for protein in the absence (dotted bar, basal; angled stripes, stimulated) or presence (□ basal; ■ stimulated) of 0.01% (w/v) CHS. The dashed lines represent the ATPase activity of ABCB1 in the absence (lower) or presence (upper) of nicardipine.

ABCA4 was examined. ABCA4 activity was measured on freshly purified protein (i.e. immediately post-metal affinity chromatography) using a sensitive [^{32}P]-ATP based assay. Purification of ABCA4 in the absence of any lipid additive caused a complete inactivation of the ATPase activity of the protein, although in all cases saturable and displaceable [γ^{32}P]-8N_3-ATP binding was still observed (data not shown). This is presumably due to the effects of FC-16 on the protein directly, or through delipidation during the chromatographic steps. The inclusion of asolectin, pure phosphatidyl-choline or a mixture of *E. coli* crude lipid extract and cholesterol (4:1 w/w) failed to provide any protection from this inactivation. This is in contrast to the ability of the two crude lipid mixtures to improve the structural stability of ABCA4.

ABCA4 is located within disc membranes of photoreceptor cells and these specialised organelles contain distinct lipid profiles. In particular, the discs have increased proportions of phosphatidyl-ethanolamine, an abundance of long chain polyunsaturated constituent fatty acids and, as they migrate towards the disc tip, lower amounts of cholesterol. To provide an approximation of this lipid environment, ABCA4 was purified in the presence of brain PE exclusively or with a crude brain extract.

In the presence of crude brain lipid extracts, the maximal activity in the absence of substrate (i.e. basal) was determined as V_{MAX} = 128 ± 16 nmol/min/mg, with an affinity constant of K_M (ATP) = 2.7 ± 0.5 mM (Table 1). The inclusion of brain PE also supported ATPase activity (V_{MAX} = 138 ± 12 nmol/min/mg) that was indistinguishable from the crude brain lipid mixture.

Retinol and retinal did not lead to significant stimulation of ATPase activity of ABCA4 in any of the lipid mixtures. Previous reports of stimulation of ATP hydrolysis by these compounds resulted in only relatively minor increases in the basal activity (~1.25 fold). As shown in Table 1, beryllium fluoride and the non-hydrolysable ATP analogue AMP-PNP were able to inhibit the basal rate of ATP hydrolysis.

Inclusion of cholesterol has been demonstrated to improve rates of ATP hydrolysis for a number of ABC proteins and was added to the crude brain mixture in a ratio of 1:4 (w/w). However, this supplementation caused a statistically significant ($P < 0.05$) 60% reduction in the basal ATPase activity to V_{MAX} = 53 ± 6 nmol/min/mg. Intriguingly, the other major protein component of disc membranes, rhodopsin, is also inhibited by cholesterol.

Clearly, the structural integrity ABCA4 and its function are heavily reliant on the presence of a specific lipid environment. Unfortunately, the GPC profiles indicate that the inclusion of lipids lead to greater heterogeneity in the sample. In order to resolve this apparent dichotomy we used electron microscopy to examine the nature of purified ABCA4 (Section 3.11).

Table 1
Activity of ABCA4 at each stage of purification; effects of lipids. ABCA4 was purified in the presence of three distinct lipid mixtures; (i) brain PE, (ii) a crude brain lipid mixture or (iii) crude brain lipid mixture in the presence of 20% (mol/mol) of cholesterol. ATPase activity was characterised at distinct ATP concentrations to generate parameters of maximal activity (V_{MAX}) and affinity for substrate (K_M) through non-linear least squares regression of the Michaelis–Menten equation. ABCA4 purified in a crude brain lipid mixture was also examined at a fixed ATP concentration (2 mM) in the presence of varying concentrations of beryllium fluoride or AMP-PNP. The extent of ATPase activity remaining (EXT) and the potency to inhibit hydrolysis (IC_{50}) were obtained using non-linear regression of the general dose–response relationship. Values correspond to mean ± SEM and were obtained from at least four independent observations.

	Brain PE	Crude brain	Crude brain + cholesterol
Activity			
V_{MAX} (nmol/min/mg)	138 ± 12	128 ± 16	53 ± 6
K_M (mM)	4.5 ± 0.9	2.7 ± 0.5	1.7 ± 0.2
Be_x·F inhibition			
Extent		0.55 ± 0.03	
IC_{50} (mM)		0.83 ± 0.17	
AMP-PNP inhibition			
Extent		0.55 ± 0.03	
IC_{50} (mM)		0.83 ± 0.17	

3.11. Electron microscopy based structural studies of ABCA4

Transmission electron microscopy (TEM) is a powerful diagnostic tool in assessing the potential suitability of a protein preparation for 2D and 3D crystallisation trials for several reasons. Firstly, an initial benefit of screening using TEM is that small scale trial preparations and low protein concentrations can be readily accommodated — a typical negative staining TEM experiment may require 10 μl of sample at a concentration of 25–50 μg/ml, whilst a 3D crystallographic screen may use a similar volume but requires a protein concentration perhaps 200× higher. Secondly, electron microscopy (EM) can provide data on "structural purity", a term that we use to encompass sample homogeneity and mono-dispersity, aggregation state, and the stability of a specific conformation.

Finally, routine screening of repeat samples by TEM allows assessment of problems that may arise from batch-to-batch variability. The negatively stained ABCA4 sample (Fig. 8a) clearly showed that the ABCA4 protein was present as a mono-disperse population of particles measuring ~110–150 Å. There was no significant detergent background or particle aggregation, although particles were closely packed on the carbon support film. The particles also ranged in shape from globular/oval to sandwich like double-layered indicating that the protein had naturally adhered to the support grid in a variety of views. Previous TEM studies on detergent solubilised ABC proteins have reported a variety of oligomeric forms and sizes. With these previous data in mind, and given that the ABCA4 topology prediction [27] indicated significant extra mass beyond the TMDs, our initial expectation was to expect a particle that was perhaps oligomeric and up to ~200 Å in the longest dimension.

EMAN2 was used to select 5300 well separated particles (Fig. 8b) and following iterative-MSA class averaging [34], produced crisp projection averages with a clear match to the raw data. These projection maps (Fig. 8c) corresponded to different projection averages of the protein, with some classes presenting a skewed toroidal projection and others a much more sandwich-like particle with a pseudo-mirror symmetry axis.

3.12. Interpretation of the 3-D structure of ABCA4

The final 3-D volume of the ABCA4 complex had dimensions of 140 × 150 × 110 Å^3, and is a consistent volume to fit a dimer of ABCA4 molecules (2 × 240 kDa) along with their associated detergent micelles (~70 kDa [38]; Fig. 8d). Using the high-resolution structure of Sav1866 (low pass filtered to 20 Å) as an approximation of the TMD and NBD regions of the ABCA4 protein, regions of density with a high correlation (0.91 at 26 Å resolution) can be identified and only have one consistent orientation. Viewed from the side in surface render (Fig. 8d), the dimeric complex has a rounded pentagonal star appearance, with the putative NBDs and TMD domains forming the outside corners of the star. There is considerable additional density located at the apex of the complex and at the interface of the two monomeric proteins the electron density for these portions of the map overlaps, was much less well-defined at lower σ values and more variable than the other map densities. To clarify the interpretation of the structure, we segmented the 3-D volume into each half of the dimeric complex, shown in the lower panels of Fig. 8d. By removing the front monomer, we are able to assign three structural "lobes" to the rendered surface. These have been putatively assigned these as the TMD (blue), NBD (green) and extracellular domains (ECD) (magenta) regions of ABCA4 (Fig. 8d, bottom panel). The ECDs of ABCA4 are predicted to form two soluble domains of 60 kDa and 30 kDa respectively, which are oriented towards the lumen of the outer segment discs. It has been suggested that disulphide bridges connect the two ECDs in ABCA proteins, and these bridges are essential for their function [27,39]. Since the ECDs are believed to be crosslinked [11], it is reasonable to assume that the density for these regions in the EM map would be contiguous; based

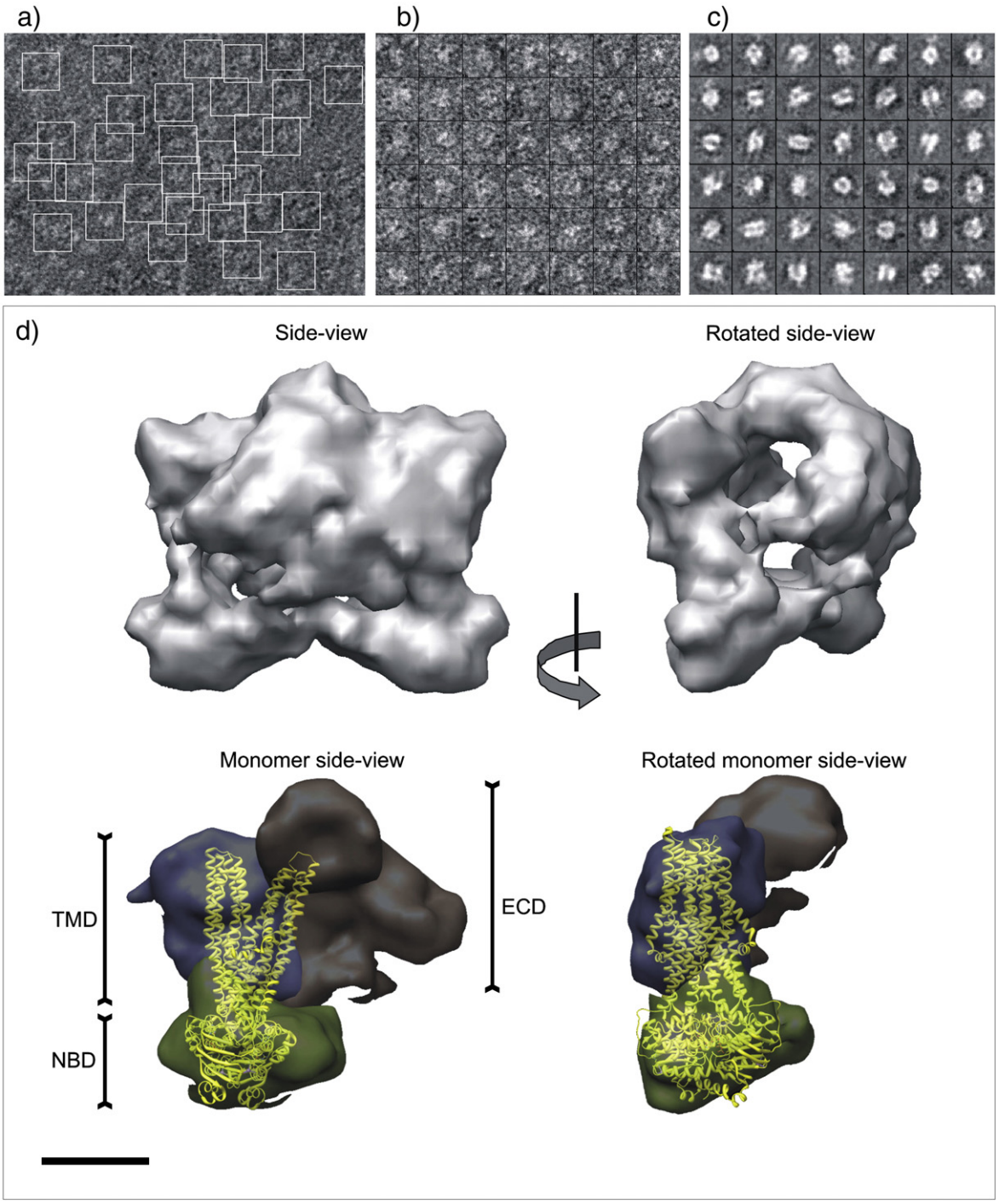

Fig. 8. 3-D Structural analysis of ABCA4 by electron microscopy and single particle analysis. CCD images of negatively-stained detergent solubilised ABCA4 (a) were recorded and showed clear oligomeric protein particles of ~13–16 nm — Scale bar = 100Å. Individual particles were selected from these micrographs into 64 pixel^2 boxes (b) and sorted into different orientation classes using iterative MSA (c). 3D reconstruction using EMAN2 produced a 26 Å resolution electron density map of the protein (two side views shown in d). The map consisted of two groups of three domains (coloured in green, blue and magenta), consistent with a dimer of ABCA4, each half consisting of a transmembrane domain (TMD), two nucleotide binding domains (NBDs) and two extra-cytoplasmic domains (ECDs). One half of the map is shown with the high resolution structure of Sav1866 (yellow) fitted into the TMD/NBD region using Chimera.

on the distribution of volume in the complex, we suggest that the remaining density, approximately one third of the total volume and a total of 4.36×10^5 Å^3, must contain the ECDs. It is interesting to note, that these regions did not project directly out beyond the TMD region and appeared to loop around and form extensive contacts with the hydrophobic TMD region.

During preparation of this manuscript a publication from Tybovsky et al. generated an electron microscopy based structure for ABCA4 [40]. The data was produced using some different methodology and highlighted some obvious structural differences to the data produced here. Tsybovsky et al. purified ABCA4 from Bovine outer rod membranes using DDM as their detergent of choice and subsequently used the random conical tilt method on a dataset of ~25 K of particles; the resulting 3-D structure from sharp projection averages was at a reported resolution of 18 Å. Firstly, the data produced by Tsybovsky et al. clearly shows a monomeric organisation of ABCA4 in contrast to the dimer produced

here. There are several examples in the literature of detergent induced oligomerisation [41] and of membrane proteins existing in multiple promiscuous oligomers [42]. In this case it is difficult to unambiguously state which has the 'more correct' in vivo relevance, unless a structure is calculated from the lipid bilayer directly. Comparing the two monomer structures, the overall size and distribution of domains is very similar, although in the data we produce the ECDs within the dimer are folded inwards towards the dimer interface. Whilst we believe this packing organisation is likely to have no physiological significance, it is interesting to note the monomeric structure of ABCA4 is much more rigid in comparison. Clearly in the case of ABCA4, the choice of detergent affects not only the purified oligomeric state, but also the flexibility and conformation of the protein produced.

4. Discussion

Our ongoing research focus is to reveal the molecular mechanisms underlying trans-membrane translocation by eukaryotic ABC proteins. The strategy combines biochemical, biophysical and structural studies of purified transporters, which necessitates the production of purified transporters at a high yield.

Sufficient expression of ABCB1 and ABCA4 has been achieved through the infection of insect cells using recombinant baculovirus. Poly-histidine tags engineered into both proteins enabled their rapid purification by IMAC. GPC, an iso-thermal stability assay, and (for ABCA4) EM techniques have been used to iteratively refine the purification procedures, improve the yield and optimise the sample homogeneity. The most significant improvements have resulted from optimising buffer components throughout the process. These improvements in protein homogeneity also contributed to improvements in the ATPase activity of both transporters in a detergent micelle matrix. Finally, the use of EM has also generated structural data for ABCA4.

Embarking on structural or biophysical studies with membrane proteins requires judicious choice of expression system. Although expression in *E. coli* is a popular first choice for many investigators there can be serious issues with folding, stability, and assembly of large membrane proteins [43–45]. Insect cells were chosen ahead of yeast expression due to prior laboratory experience, their ability to mediate core glycosylation [46–48] and provide a phospholipid environment more similar to mammalian cells [49] though the membrane sterols in both yeast and insect cells differ from those in mammalian cells [45].

Extraction of proteins from the source membranes is a frequent "bottleneck" in the isolation of membrane transporters [44,50]. The general physical properties of detergents including their alkyl chain length, CMC, and the size or charge of the polar head group, can indicate their ability to solubilise membrane proteins. However, it remains impossible to accurately predict the ability of each detergent to solubilise a specific protein. For instance, previous studies have demonstrated that ABCB1 is readily extracted from insect and mammalian cell membranes using a variety of detergent classes [15,51–53]. By contrast, ABCA4 was difficult to extract from Sf9 insect cell membranes; only the long-chain zwitterionic fos-cholines were able to solubilise the protein. This observation was reiterated in our laboratory for ABCG2 [27] and there are numerous other examples where the fos-cholines provided improved extraction of membrane proteins [5,54–56]; however there are scant reports of their effects on protein activity.

Another ABC transporter, the prokaryotic BmrC/D transporter also proved difficult to extract from membranes and repeatedly formed higher order aggregates following purification [57]. Here again, shortening the time for protein production (i.e. post-infection of insect cells with baculovirus) lowered the overall final yield but significantly reduced the degree of BmrC/D aggregation. Our experience indicates that increasing the period of baculovirus infection provided considerably greater yield for ABCB1 and ABCA4, but at a cost of reduced "extractability". This fraction of "late-stage" insoluble protein may reflect an increased amount of mis-folded protein, or may reflect membrane protein aggregation within the membrane itself resulting in limiting exposure to detergents during solubilisation [43,44,58,59]. Such a scenario may limit extraction of the protein or lead to extraction of proteins in an oligomeric configuration.

It is clear that the optimal detergent for extraction may not be suitable for down-stream applications such as functional assessment or crystallisation [5,44]. For instance detergents with low CMCs may be difficult to remove during reconstitution, and long alkyl chains may be more disruptive to crystal contacts. As indicated from our investigations with several ABC transporters, even related proteins may have distinct extraction profiles. In addition, the specific cellular membrane environment will also influence extraction. However, the extracting detergent may be substituted for one that supports downstream analysis during chromatographic purification [55].

Successful structural determination of membrane proteins requires protein samples that are not only pure but also monodisperse. Using GPC, we identified high molecular weight species migrating in the void volume of the GPC columns, which indicated the presence of aggregated species. These ABC transporters may form aggregates within the insect cells during the protein production phase following infection with recombinant baculovirus. Alternatively the appearance of ABCB1 or ABCA4 aggregates following purification may result directly from the process of extraction by detergent.

Buffer composition is an oft-ignored, or relegated to "bystander", influence on the stability and integrity of purified proteins. Yet as several authors have shown, the influence of pH, glycerol content and ionic strength on the aggregation state of a number of membrane proteins [29,30,60], including ABCB1 [61], vary from case to case. Here, we observed that the cholesterol derivative (cholesteryl hemi-succinate) was shown to provide considerable stability to detergent soluble ABCB1 against thermal denaturation and reduced the high molecular weight shoulder peak in the gel permeation chromatography spectrum. This suggests that the cholesterol derivative may prevent the formation of ABCB1 aggregates in the mixed micelle suspensions. The inclusion of CHS allowed drug stimulated ATPase activity to be retained by ABCB1 in the detergent solubilised state, in contrast to previous observations with detergent soluble ABCB1 [15,36,62]. The "protective" effect of CHS agrees with an earlier investigation using reconstituted ABCB1 [61]. We suggest that this effect is due to CHS conferring a reduction in fluidity to the micelle in the same way that cholesterol and sphingolipid-mediated ordering of the membrane is conducive to optimal activity of reconstituted ABCB1 [21,36].

Our analysis of buffer components also revealed that these can influence the aggregation and precipitation of protein during purification and concentration. As previously described, centrifugal concentrators can result in aggregation or precipitation of membrane proteins [58]. We observed that this was compounded by the presence of eluting concentrations of imidazole, as revealed by the GPC profiles. The removal of imidazole both improved the GPC profile, and reduced the extent of protein precipitation during centrifugal concentration, yielding protein samples in the range 10–15 mg/ml. However, in the case of ABCA4, for the protein to reach a high concentration without aggregation, it also required the right detergent.

The isothermal denaturation assay identified lipid additives that improved the stability of ABCA4 solubilised by fos-choline detergents and the highest stability was afforded by the crude lipid mixtures asolectin and *E. coli* lipids. Asolectin comprises approximately equal proportions of PC, PE and PI with a distribution of alkyl chain lengths and degrees of saturation. The *E. coli* lipid extract comprises 58% PE, 15% PG and 10% cardiolipin, also with a range of alkyl chain properties. In contrast the use of egg-PC, which contains a single lipid head group, was not able to improve ABCA4 stability. The crude mixtures are unlikely to provide an ordered lipid environment per se, but their inclusion is likely to render the mixed micelles more rigid than detergent alone [63–66].

The two crude lipid mixtures that provided thermal stability to ABCA4 contain relatively high amounts of PE. A wide range of lipid

species was examined for their ability to sustain ATPase activity of purified ABCA4 and optimal function was obtained in brain PE and crude brain lipids (33% PE, 12% C, and 19% PS). Clearly, a high proportion of PE is a key lipid in the functional and structural integrity of ABCA4. In addition, these two lipid mixtures also contain a high proportion of long and highly unsaturated alkyl chains (Brain PE: 24% 18:1, 12% 22:6, and 19% 20:4). PE has a small head group in relation to other natural lipids and is unable to form conventional bilayers on its own. Thus, the combination of PE and highly unsaturated lipids precludes the formation of highly ordered lipid domains. However, ABCA4 in pure micelles of fos-choline, and therefore disordered, is void of functional activity. This would suggest that a direct interaction between PE-based lipid species and ABCA4 is crucial to the protein's integrity.

The advent of heterologous expression systems and affinity tags has facilitated the production of highly purified and stable membrane proteins; a task that has long been viewed as very challenging. Our experience in these systems has led us to establish the following recommendations for any novel membrane protein purification protocol. Firstly, in order to produce both functional and structurally pure samples, a critical assessment of the protein stability or homogeneity should be undertaken prior to functional or structural investigations, since each additional stage of the laborious purification procedure has the ability to reduce both protein quality and quantity. Relating to this, we would initially suggest a series of empirical observations on the effects of detergents, lipids and buffer components on the purification, since these factors can have a large effect on protein stability but are relatively easily refined. Moreover, a range of assays to examine the protein stability, such as GPC and thermal stability assays should then be employed since they will generate distinct datasets. Finally, the functional activity of membrane transporters will correlate strongly with the integrity of the purified product, a vital consideration for undertaking structural studies. That said, in this case, we have an interesting caveat since following removal from the membrane bilayer the single particle structure of ABCA4 has revealed an unusual quaternary organisation. Here, we would suggest that during purification the ECDs of the protein have packed stably into the side of the complex and for this to have occurred, the ECDs would have to represent a highly mobile hinged domain or a naturally disordered region of the protein in vivo. These structural data suggest that despite its high purity, stable nature and monodispersity, ABCA4 purified in this way may represent a non-ideal conformation to pursue a 3-D crystallisation route. Screening further conditions to stabilise the ECDs (e.g. crosslinking using the GRAFIX method [67] or co-purification with ligand bound) would perhaps yield a preparation that more reflects the physiological organisation and optimised for 3-D crystallisation.

Acknowledgements

The work was part funded by a project grant from the Medical Research Council UK (G040063) and an EU Marie Curie Research Training Network grant (MRTN-CT-2004-005330) with a studentship awarded to PN. NLP was the recipient of an MRC departmental studentship. We thank Alison September for early work on establishing the expression and molecular biology of ABCA4.

References

[1] P.M. Jones, M.L. O'Mara, A.M. George, ABC transporters: a riddle wrapped in a mystery inside an enigma, Trends Biochem. Sci. 34 (2009) 520–531.
[2] R. Callaghan, A.M. George, I.D. Kerr, Molecular aspects of the translocation process by ABC proteins, in: H.E. Edward (Ed.), Comprehensive Biophysics, Elsevier, Amsterdam, 2012, pp. 145–173.
[3] O. Jardetzky, Simple allosteric model for membrane pumps, Nature 211 (1966) 969–970.
[4] G.G. Privé, Detergents for the stabilization and crystallization of membrane proteins, Methods 41 (2007) 388–397.
[5] S. Newstead, H. Kim, G. von Heijne, S. Iwata, D. Drew, High-throughput fluorescent-based optimization of eukaryotic membrane protein overexpression and purification in Saccharomyces cerevisiae, Proc. Natl. Acad. Sci. U. S. A. 104 (2007) 13936–13941.
[6] D. Drew, S. Newstead, Y. Sonoda, H. Kim, G. von Heijne, S. Iwata, GFP-based optimization scheme for the overexpression and purification of eukaryotic membrane proteins in *Saccharomyces cerevisiae*, Nat. Protoc. 3 (2008) 784–798.
[7] S. Newstead, S. Ferrandon, S. Iwata, Rationalizing alpha-helical membrane protein crystallization, Protein Sci. 17 (2008) 466–472.
[8] T. Warne, M.J. Serrano-Vega, C.G. Tate, G.F.X. Schertler, Development and crystallization of a minimal thermostabilised G protein-coupled receptor, Protein Expr. Purif. 65 (2009) 204–213.
[9] C.A. Shintre, A.C. Pike, Q. Li, J.I. Kim, A.J. Barr, S. Goubin, L. Shrestha, J. Yang, G. Berridge, J. Ross, P.J. Stansfeld, M.S. Sansom, A.M. Edwards, C. Bountra, B.D. Marsden, F. von Delft, A.N. Bullock, O. Gileadi, N.A. Burgess-Brown, E.P. Carpenter, Structures of ABCB10, a human ATP-binding cassette transporter in apo- and nucleotide-bound states, Proc. Natl. Acad. Sci. U. S. A. 110 (2013) 9710–9715.
[10] S.G. Aller, J. Yu, A. Ward, Y. Weng, S. Chittaboina, R. Zhuo, P.M. Harrell, Y.T. Trinh, Q. Zhang, I.L. Urbatsch, G. Chang, Structure of P-glycoprotein reveals a molecular basis for poly-specific drug binding, Science 323 (2009) 1718–1722.
[11] M.S. Jin, M.L. Oldham, Q. Zhang, J. Chen, Crystal structure of the multidrug transporter P-glycoprotein from *Caenorhabditis elegans*, Nature 490 (2012) 566–569.
[12] N. Kartner, J.R. Riordan, V. Ling, Cell surface P-glycoprotein associated with multidrug resistance in mammalian cell lines, Science 221 (1983) 1285–1288.
[13] J.R. Riordan, K. Deuchars, N. Kartner, N. Alon, J. Trent, V. Ling, Amplification of P-glycoprotein genes in multidrug-resistant mammalian cell lines, Nature 316 (1985) 817–819.
[14] L.J. Goldstein, A.T. Fojo, K. Ueda, W. Crist, A. Green, G. Brodeur, I. Pastan, M.M. Gottesman, Expression of the multidrug resistance, MDR1, gene in neuroblastomas, J. Clin. Oncol. 8 (1990) 128–136.
[15] E. Crowley, M.L. O'Mara, I.D. Kerr, R. Callaghan, Trans-membrane helix 12 plays a pivotal role in coupling energy provision and drug binding in ABCB1, FEBS J. 277 (19) (2010) 3974-85.
[16] A. Heikal, K. Box, A. Rothnie, J. Storm, R. Callaghan, M. Allen, The stabilisation of purified, reconstituted P-glycoprotein by freeze drying with disaccharides, Cryobiology 58 (2009) 37–44.
[17] C. Martin, G. Berridge, C.F. Higgins, P. Mistry, P. Charlton, R. Callaghan, Communication between multiple drug binding sites on P-glycoprotein, Mol. Pharmacol. 58 (2000) 624–632.
[18] C.A. McDevitt, C.A. Shintre, G.J. Grossmann, N.L. Pollock, S.M. Prince, R. Callaghan, R.C. Ford, Structural insights into P-glycoprotein (ABCB1) by small angle X-ray scattering and electron crystallography, FEBS Lett. 582 (2008) 2950–2956.
[19] A.M. Taylor, J. Storm, L. Soceneantu, K.J. Linton, M. Gabriel, C. Martin, J. Woodhouse, E. Blott, C.F. Higgins, R. Callaghan, Detailed characterization of cysteine-less P-glycoprotein reveals subtle pharmacological differences in function from wild-type protein, Br. J. Pharmacol. 134 (2001) 1609–1618.
[20] E. Crowley, M.L. O'Mara, C. Reynolds, D.P. Tieleman, J. Storm, I.D. Kerr, R. Callaghan, Transmembrane helix 12 modulates progression of the ATP catalytic cycle in ABCB1, Biochemistry 48 (2009) 6249–6258.
[21] A. Rothnie, D. Theron, L. Soceneantu, C. Martin, M. Traikia, G. Berridge, C.F. Higgins, P.F. Devaux, R. Callaghan, The importance of cholesterol in maintenance of P-glycoprotein activity and its membrane perturbing influence, Eur. Biophys. J. 30 (2001) 430–442.
[22] M.F. Rosenberg, R. Callaghan, R.C. Ford, C.F. Higgins, Structure of the multidrug resistance P-glycoprotein to 2.5 nm resolution determined by electron microscopy and image analysis, J. Biol. Chem. 272 (1997) 10685–10694.
[23] M.F. Rosenberg, R. Callaghan, S. Modok, C.F. Higgins, R.C. Ford, Three-dimensional structure of P-glycoprotein: the transmembrane regions adopt an asymmetric configuration in the nucleotide-bound state, J. Biol. Chem. 280 (2005) 2857–2862.
[24] M.F. Rosenberg, G. Velarde, R.C. Ford, C. Martin, G. Berridge, I.D. Kerr, R. Callaghan, A. Schmidlin, C. Wooding, K.J. Linton, C.F. Higgins, Repacking of the transmembrane domains of P-glycoprotein during the transport ATPase cycle, EMBO J. 20 (2001) 5615–5625.
[25] R. Allikmets, N.F. Shroyer, N. Singh, J.M. Seddon, R.A. Lewis, P.S. Bernstein, A. Peiffer, N.A. Zabriskie, Y. Li, A. Hutchinson, M. Dean, J.R. Lupski, M. Leppert, Mutation of the Stargardt disease gene (ABCR) in age-related macular degeneration, Science 277 (1997) 1805–1807.
[26] H. Sun, J. Nathans, Stargardt's ABCR is localized to the disc membrane of retinal rod outer segments, Nat. Genet. 17 (1997) 15–16.
[27] S. Bungert, L.L. Molday, R.S. Molday, Membrane topology of the ATP binding cassette transporter ABCR and its relationship to ABC1 and related ABCA transporters: identification of N-linked glycosylation sites, J. Biol. Chem. 276 (2001) 23539–23546.
[28] J. Storm, M.L. O'Mara, E.H. Crowley, J. Peall, D.P. Tieleman, I.D. Kerr, R. Callaghan, Residue G346 in transmembrane segment six is involved in inter-domain communication in P-glycoprotein, Biochemistry 46 (2007) 9899–9910.
[29] Y. Sonoda, S. Newstead, N.J. Hu, Y. Alguel, E. Nji, K. Beis, S. Yashiro, C. Lee, J. Leung, A.D. Cameron, B. Byrne, S. Iwata, D. Drew, Benchmarking membrane protein detergent stability for improving throughput of high-resolution X-ray structures, Structure 19 (2011) 17–25.
[30] A.I. Alexandrov, M. Mileni, E.Y.T. Chien, M.A. Hanson, R.C. Stevens, Microscale fluorescent thermal stability assay for membrane proteins, 16 (2008) 351–359.
[31] S. Chifflet, U.T.R. Chiesa, S. Tolosa, A method for the determination of inorganic phosphate in the presence of labile organic phosphate and high concentrations of protein: application to lens ATPases, Anal. Biochem. 168 (1988) 1–4.
[32] R.F. Collins, T.D. Flint, A. Holzenburg, R.C. Ford, Structural changes in photosystem II after treatment with the zero-length bifunctional cross-linker 1-ethyl-3-(3-dimethylaminopropyl)carbodi-imide: an electron microscopic study, Biochem. J. 319 (Pt 2) (1996) 585–589.

[33] R.F. Collins, L. Davidsen, J.P. Derrick, R.C. Ford, T. Tonjum, Analysis of the PilQ secretin from *Neisseria meningitidis* by transmission electron microscopy reveals a dodecameric quaternary structure, J. Bacteriol. 183 (2001) 3825–3832.
[34] S.J. Ludtke, P.R. Baldwin, W. Chiu, EMAN: semiautomated software for high-resolution single-particle reconstructions, J. Struct. Biol. 128 (1999) 82–97.
[35] C.A. McDevitt, R. Collins, I.D. Kerr, R. Callaghan, Purification and structural analyses of ABCG2, Adv. Drug Deliv. Rev. 61 (2009) 57–65.
[36] S. Modok, C. Heyward, R. Callaghan, P-glycoprotein retains function when reconstituted into a sphingolipid- and cholesterol-rich environment, J. Lipid Res. 45 (2004) 1910–1918.
[37] R. Callaghan, G. Berridge, D.R. Ferry, C.F. Higgins, The functional purification of P-glycoprotein is dependent on maintenance of a lipid–protein interface, Biochim. Biophys. Acta 1328 (1997) 109–124.
[38] P. Strop, A.T. Brunger, Refractive index-based determination of detergent concentration and its application to the study of membrane proteins, Protein Sci. 14 (2005) 2207–2211.
[39] M. Hozoji, Y. Kimura, N. Kioka, K. Ueda, Formation of two intramolecular disulfide bonds is necessary for ApoA-I-dependent cholesterol efflux mediated by ABCA1, J. Biol. Chem. 284 (2009) 11293–11300.
[40] Y. Tsybovsky, T. Orban, R.S. Molday, D. Taylor, K. Palczewski, Molecular organization and ATP-induced conformational changes of ABCA4, the photoreceptor-specific ABC transporter, Structure 21 (2013) 854–860.
[41] R.C. Ford, A. Holzenburg, Investigation of the structure of trimeric and monomeric photosystem I reaction centre complexes, EMBO J. 7 (1988) 2287–2293.
[42] K. Larue, R.C. Ford, L.M. Willis, C. Whitfield, Functional and structural characterization of polysaccharide co-polymerase proteins required for polymer export in ATP-binding cassette transporter-dependent capsule biosynthesis pathways, J. Biol. Chem. 286 (2011) 16658–16668.
[43] N. Eifler, M. Duckely, L.T. Sumanovski, T.M. Egan, A. Oksche, J.B. Konopka, A. Luthi, A. Engel, P.J. Werten, Functional expression of mammalian receptors and membrane channels in different cells, J. Struct. Biol. 159 (2007) 179–193.
[44] I. Mus-Veteau, Heterologous expression of membrane proteins for structural analysis, Methods Mol. Biol. 601 (2010) 1–16.
[45] C.G. Tate, Overexpression of mammalian integral membrane proteins for structural studies, FEBS Lett. 504 (2001) 94–98.
[46] T.P. Knepper, B. Arbogast, J. Schreurs, M.L. Deinzer, Determination of the glycosylation patterns, disulfide linkages, and protein heterogeneities of baculovirus-expressed mouse interleukin-3 by mass spectrometry, Biochemistry 31 (1992) 11651–11659.
[47] X. Shi, D.L. Jarvis, Protein N-glycosylation in the baculovirus-insect cell system, Curr. Drug Targets 8 (2007) 1116–1125.
[48] A. Bernard, M. Payton, K.R. Radford, Protein expression in the baculovirus system, Curr. Protoc. Protein Sci. (2001) 5(Chapter 5, Unit5).
[49] K. Marheineke, S. Grunewald, W. Christie, H. Reilander, Lipid composition of *Spodoptera frugiperda* (Sf9) and *Trichoplusia ni* (Tn) insect cells used for baculovirus infection, FEBS Lett. 441 (1998) 49–52.
[50] C.A. McDevitt, R. Callaghan, How can we best use structural information on P-glycoprotein to design inhibitors? Pharmacol. Ther. 113 (2007) 429–441.
[51] I.L. Urbatsch, M.K. Al-Shawi, A.E. Senior, Characterization of the ATPase activity of purified Chinese hamster P-glycoprotein, Biochemistry 33 (1994) 7069–7076.
[52] T.W. Loo, D.M. Clarke, Rapid purification of human P-glycoprotein mutants expressed transiently in HEK 293 cells by nickel-chelate chromatography and characterization of their drug stimulated ATPase activities, J. Biol. Chem. 270 (1995) 21449–21452.
[53] F.J. Sharom, X. Yu, C.A. Doige, Functional reconstitution of drug transport and ATPase activity in proteoliposomes containing partially purified P-glycoprotein, J. Biol. Chem. 268 (1993) 24197–24202.
[54] B.T. Arachea, Z. Sun, N. Potente, R. Malik, D. Isailovic, R.E. Viola, Detergent selection for enhanced extraction of membrane proteins, Protein Expr. Purif. 86 (2012) 12–20.
[55] P. Curnow, L. Senior, M.J. Knight, K. Thamatrakoln, M. Hildebrand, P.J. Booth, Expression, purification, and reconstitution of a diatom silicon transporter, Biochemistry 51 (2012) 3776–3785.
[56] D. Russell, O. Kolaj-Robin, T. Soulimane, *Maricaulis maris* cation diffusion facilitator: achieving homogeneity through a mixed-micelle approach, Protein Expr. Purif. 85 (2012) 173–180.
[57] C. Galian, F. Manon, M. Dezi, C. Torres, C. Ebel, D. Levy, J.M. Jault, Optimized purification of a heterodimeric ABC transporter in a highly stable form amenable to 2-D crystallization, PLoS One 6 (2011) e19677.
[58] I. Maslennikov, M. Krupa, C. Dickson, L. Esquivies, K. Blain, G. Kefala, S. Choe, W. Kwiatkowski, Characterization of protein detergent complexes by NMR, light scattering, and analytical ultracentrifugation, J. Struct. Funct. Genomics 10 (2009) 25–35.
[59] S. Ravaud, M.A. Do Cao, M. Jidenko, C. Ebel, M. Le Maire, J.M. Jault, A. Di Pietro, R. Haser, N. Aghajari, The ABC transporter BmrA from *Bacillus subtilis* is a functional dimer when in a detergent-solubilized state, Biochem. J. 395 (2006) 345–353.
[60] V.L. Postis, S.E. Deacon, P.C. Roach, G.S. Wright, X. Xia, J.C. Ingram, J.M. Hadden, P.J. Henderson, S.E. Phillips, M.J. McPherson, S.A. Baldwin, A high-throughput assay of membrane protein stability, Mol. Membr. Biol. 25 (2008) 617–624.
[61] A. Kodan, H. Shibata, T. Matsumoto, K. Terakado, K. Sakiyama, M. Matsuo, K. Ueda, H. Kato, Improved expression and purification of human multidrug resistance protein MDR1 from baculovirus-infected insect cells, Protein Expr. Purif. 66 (2009) 7–14.
[62] C.A. Doige, X. Yu, F.J. Sharom, The effects of lipids and detergents on ATPase-active P-glycoprotein, Biochim. Biophys. Acta 1146 (1993) 65–72.
[63] M. Hattori, R.E. Hibbs, E. Gouaux, A fluorescence-detection size-exclusion chromatography-based thermostability assay for membrane protein precrystallization screening, Structure 20 (2012) 1293–1299.
[64] R. Mancusso, N.K. Karpowich, B.K. Czyzewski, D.N. Wang, Simple screening method for improving membrane protein thermostability, Methods 55 (2011) 324–329.
[65] R. Saxena, A. Chattopadhyay, Membrane cholesterol stabilizes the human serotonin(1A) receptor, Biochim. Biophys. Acta 1818 (2012) 2936–2942.
[66] B. Zehnpfennig, I.L. Urbatsch, H.J. Galla, Functional reconstitution of human ABCC3 into proteoliposomes reveals a transport mechanism with positive cooperativity, Biochemistry 48 (2009) 4423–4430.
[67] H. Stark, GraFix: stabilization of fragile macromolecular complexes for single particle cryo-EM, Methods Enzymol. 481 (2010) 109–126.